Journal of Applied Polymer Science

Tough Hyperbranched Epoxy/Poly(amido-amine) Modified Bentonite Thermosetting Nanocomposites

Bibekananda De, Niranjan Karak
Advanced Polymer and Nanomaterial Laboratory, Department of Chemical Sciences, Tezpur University, Napaam, Assam, India
Correspondence to: N. Karak (E-mail: karakniranjan@yahoo.com)

ABSTRACT: A tough and highly flexible hyperbranched epoxy and poly(amido-amine) modified bentonite based thermosetting nanocomposite was demonstrated. The FTIR, XRD, and TGA analyses confirmed the modification of bentonite. The formation of partially exfoliated structure of the nanocomposite with good physicochemical interactions among the hyperbranched epoxy, poly(amido-amine) hardener and modified clay was investigated by the FTIR, XRD, SEM, and TEM analyses. Significant improvements of 750% toughness, 300% elongation at break, 50% tensile strength, 300% modulus, and 250% adhesive strength of the pristine epoxy were achieved by the formation of nanocomposites with 3 wt % of modified clay. The experimental modulus values of the nanocomposites were compared with three theoretical models to account the interactions between filler and matrix. Thus, the studied epoxy nanocomposite has great potential to be used as an advanced epoxy thermoset. © 2014 Wiley Periodicals, Inc. J. Appl. Polym. Sci. **2014**, *131*, 40327.

KEYWORDS: nanostructured polymers; clay; thermosets

Received 2 November 2013; accepted 17 December 2013
DOI: 10.1002/app.40327

INTRODUCTION

Epoxy thermosets are widely used as high performance engineering materials, due to their good mechanical strength, dimensional stability, and chemical resistance. But their low toughness and hence high brittleness character restrict the service requirements in many advanced applications.[1–4] Recently hyperbranched epoxy achieved significant attention with their unique advantages, which include low solution and shear viscosity, high solubility in different solvents and high reactivity.[4–7] However, because of their poor mechanical strength, it is difficult to attain the desired performance of the resulted thermosets. However, through the proper molecular engineering using combination of aromatic and aliphatic moieties can improve the desired strength and toughness, as shown in our recent report.[1] In addition to this, the literatures over two decades confirmed the enhancement of desired performance of many polymers including epoxy by the formation of their suitable nanocomposites using appropriate nanomaterials.[4,8–10] Among all such nanomaterials, organically modified hydrophobic clay is widely studied because of its layer structure with high aspect ratio, which allows efficient load tolerance of the matrix.[11–14] The basic principle for the improvement in performance of these polymer/clay nanocomposites is penetration and interaction of the polymer chains within the interlayer galleries of clay. In contrary, hydrophilic nature of the unmodified clay resulted high moisture absorption and incompatibility with the hydrophobic polymer matrix. Thus, different methods have been reported to make it hydrophobic for good dispersion in the polymer matrices.[15–19] Alkylammonium cation exchange is a very common process among them use to make hydrophobic clay for preparation of polymer nanocomposites. However, it has been observed in most of the literatures, such polymer/clay nanocomposites significantly improved only tensile strength, modulus, flexural strength, and hardness. However, the desired flexibility, toughness, and elongation at break are rare to achieve in all such cases.[20,21] It is pertinent to mention here that the reports on modified clay/epoxy nanocomposites with improvement of fracture toughness, modulus and in few cases tensile strength are found in literature. Wang et al. reported epoxy nanocomposites with highly exfoliated clay where improvements of 80% stress intensity factor (K_{IC}), 190% critical strain energy release (G_{IC}) and 40% modulus were found with 2.5 wt % slurry clay.[13] The organoclay modified epoxy nanocomposites with improvements of 80% K_{IC}, 152% G_{IC}, and 20% modulus at 12 phr organoclay was reported Liu et al.[22] Zerda et al. reported intercalated clay/epoxy nanocomposites with 100% improvement in K_{IC} and G_{IC} was found at 3.5 wt % clay.[23] A epoxy/nanoclay composite with 50% enhancement in tensile strength, 77% improvement in K_{IC} and 190% increment in G_{IC} at 2 wt % clay was reported by Wang et al.[24] However, in all the above cases, a decrease in elongation at break or both elongation at break and tensile strength up to 50% and thus a massive reduction in ductility was observed. Balakrishnan et al.

also reported the increments of tensile modulus and strength though ductility decreases with the increase of organoclay content in diglycidyl ether of bisphenol-A based epoxy matrix.[25] Hence a common and serious drawback of epoxy thermoset is low ductility and hence toughness remained unsolved. Therefore, we report a simple strategy to achieve the desired tensile strength, elongation at break, toughness, and ductility of a hyperbranched epoxy nanocomposites by the incorporation of hydrophobic aliphatic poly(amido-amine) modified bentonite. In the present investigation, the modified nanoclay may toughen and flexibilize the epoxy resin because of the unique structure of the modifying agent. Further, the amalgamation of this unique structural architecture with the hyperbranched architecture of epoxy resin may provide strong physicochemical interactions among themselves.

Again, mathematical modeling plays an important role in predicting properties of a polymer nanocomposite as well as to account the different interactions between nanomaterial and polymer matrix. The incorporation of rigid platelets of clay to the polymer matrices can produce number of effects like increment of strength, stiffness, modulus, fracture toughness, etc. These increments in properties of nanocomposites are affected by number of parameters, such as shape, size, aspect ratio, volume fraction, and distribution of the reinforcing nanomaterials. In literatures a number of theories and equations have been developed to describe these phenomenon.[26–30] But here we have chosen those models which represented the best fitting of the experimental data.

An attempt has been made, therefore, to fabricate nanocomposites of a hyperbranched epoxy and an aliphatic poly(amido-amine) modified bentonite at different wt % of clay to achieve the desired strength, toughness, ductility and adhesive strength. To account the interactions between modified clay and hyperbranched epoxy, the experimental modulus values of the nanocomposites were compared with the predicting values calculated from Guth generalized Einstein equation and Halpin–Tsai random and aligned parallel models.

EXPERIMENTAL

Materials

Triethanol amine was purchased from Merck, India and was used after vacuum drying. Bisphenol-A (G. S. Chemical) was used after re-crystallized from toluene. Epichlorohydrin (Sisco Research Laboratories), methyl acrylate (G. S. Chemicals), butane 1, 4-diamine (Sigma-Aldrich), ethylene diamine (Sigma-Aldrich), hydrophilic bentonite clay (Sigma-Aldrich), sodium hydroxide (Rankem), hydrochloric acid (Merck) and poly(amido-amine) (HY840, Ciba Geigy) with amine value 5–7 eq./kg were used as received. All other reagents used were of reagent grade.

Preparation of Hyperbranched Epoxy

The hyperbranched epoxy resin was prepared by an $A_2 + B_3$ polycondensation reaction between in situ generated diglycidyl ether of bisphenol-A and triethanol amine (20 wt % of bisphenol-A) in 3 : 1 mole ratio at 110°C for 4 h using aqueous NaOH as the catalyst as reported earlier.[1] Briefly, epichlorohydrin (23.66 g, 0.2556 mol) was reacted with bisphenol-A (10.0 g, 0.0438 mol) and triethanol amine mixture (2.0 g, 0.0134 mol) at 110°C in the presence of 5 *N* aqueous NaOH solution (5.11 g, 0.1278 mol). The purified resinous final product was dried under vacuum at 70°C. The epoxy equivalent and degree of branching of the hyperbranched epoxy was 358 g/eq. and 0.79 respectively.[1] The value of shear viscosity of the prepared hyperbranched epoxy was 16–19 Pas at 25°C.

Preparation of Aliphatic Poly(amido-amine)

The aliphatic poly(amido-amine) was prepared by literature reported Michael addition reaction of amine(s) with acrylate.[31,32] Briefly, in the first step, the core moiety was prepared by the addition reaction of methanolic 1, 4-butane diamine (2 g, 0.0226 mol) with excess methyl acrylate (15.62 g, 0.18 mol) at room temperature (ca. 25°C) for 72 h. In the second step, poly(amido-amine) was prepared by addition reaction of excess methanolic ethylene diamine (0.2268 mol) with the above product at room temperature for 72 h. Excess methanol, acrylate, and amine were removed under vacuum at room temperature. The yield of the liquid purified dry product was 96%. The shear viscosity of the prepared poly(amido-amine) was found to be 0.98 Pas. The main characteristic features of FTIR and ^{13}C NMR spectra of aliphatic poly(amido-amine) are given bellow. FTIR spectrum (cm^{-1}): 1640, 3300, 2936, 1535, 1405, 1125, and 700 (amide linkage, —NH, —CH stretching, —NH, —CH_2 bending, —CN stretching, and —NH out of plane stretching frequency, respectively). ^{13}C NMR spectrum (ppm): $\delta = 162$ (amide carbon), 50 and 23 (two —CH_2 carbons of butane diamine), 42 and 30 (carbons of ethylene diamine), 46 and 33 (—CH_2 carbons of methyl acrylate attached with butane diamine and carbonyl carbon).

Modification of Bentonite Clay by Aliphatic Poly(amido-ammonium) Salt

For the modification of bentonite clay, at first the ammonium salt of aliphatic poly(amido-amine) was prepared by the treatment of 2 g of poly(amido-amine) with 18 mL of aqueous HCl (1 *N*) at 70°C for 2 h. The prepared poly(amido-ammonium) salt was slowly added to the well dispersed aqueous clay (1 g) with constant stirring at room temperature. After complete addition of the salt, the temperature of the mixture was raised up to 70°C and the conditions were maintained for another 4 h. Then the mixture was filtered and washed with water for several times for complete removal of Cl^- ions (checked by 0.1 *M* $AgNO_3$ solution). Finally, the treated clay was washed with THF for 2–3 times and then dispersed in THF (1 mL/10 mg). A little amount of this clay was dried under vacuum at 60°C for analysis.

Preparation of Hyperbranched Epoxy/Modified Clay Nanocomposites

The hyperbranched epoxy/modified clay nanocomposites were prepared by solution technique. The requisite amount (1, 3, and 5 wt %, separately) of the dispersed clay in THF was added into the hyperbranched epoxy and the mixture was stirred for 5 h followed by ultra sonication at 60% amplitude and 0.5 cycles (acoustic power density: 460 W/cm^2) for 10 min at 25–30°C. Then, 50 wt % of poly(amido-amine) was added to it and mixed homogeneously at room temperature. The mixture was

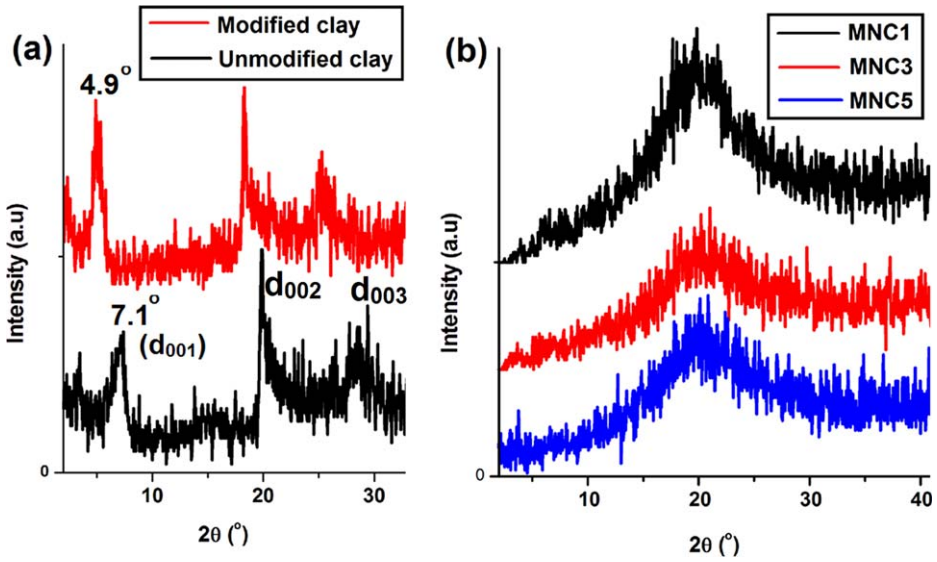

Figure 1. (a) XRD patterns of pristine and modified bentonite and (b) XRD patterns of nanocomposites. [Color figure can be viewed in the online issue, which is available at wileyonlinelibrary.com.]

coated on mild glass plates and steel plates for curing. Before curing the plates were kept under vacuum at room temperature for 24 h to remove THF. Then, the plates were cured inside the furnace at 100°C for specified time interval. The curing time was optimized by determining the swelling value. The cured nanocomposites were coded as MNC1, MNC3, and MNC5 for 1, 3, and 5 wt % modified clay, respectively. The pristine hyperbranched epoxy thermoset was coded as MNC0.

Characterization

The ultra sonication for the preparation of the hyperbranched epoxy/modified clay nanocomposites was done by ultrasonic processor (UP200S) with a standard sonotrode (tip diameter 3 mm). The FTIR spectra of the bentonite, modified bentonite, and nanocomposites were recorded on a Nicolet FTIR spectroscope (Impact-410) using KBr pellet. The crystalinity and the interlayer spacing of the clay were measured by X-ray diffractometer, Miniflex (Rigaku Corporation). The morphology of the nanocomposites was studied by high resolution transmission electron microscope, HRTEM (JEOL, JEMCXII, Transmission Electron Microscope operating voltage at 200 kV), and scanning electron microscope, SEM (JEOL, JSM-6390 LV). The tensile strength (standard ASTM D 882) and lap-shear tensile adhesive strength of the hyperbranched epoxy/modified clay nanocomposites were measured by Universal Testing Machine (UTM, WDW10). The tensile test was performed on rectangular sample (size 60 × 10 × 0.3 mm^3) with a 500 N load cell at a crosshead speed of 10 mm/min. The lap-shear adhesion test (standard ASTM D4896-01) was carried out on metal–metal (M–M) and wood–wood (W–W) adherents by lap-shear test (the area of the overlapping zone was 25 × 25 mm^2 and thickness of the zone was 0.02–0.03 mm) with a 10 kN load cell at a crosshead speed of 50 mm/min. The lap-shear tensile strength (MPa) (calculated as maximum load per unit bonded area) was obtained directly from the UTM. Scratch hardness test (standard ASTM G171) was carried out by scratch hardness tester (Sheen instrument) on the surface of hyperbranched epoxy/clay nanocomposites (area 75 × 25 × 0.3 mm^3). Impact strength of the nanocomposites was measured by Impact tester (S. C. Dey) as per the standard falling weight (ball) method (standard ASTM D 1709). The bending test of the thermosets was done using a mandrel with diameter 1–100 mm (standard ASTM D 522). All the tests for the measurement of mechanical properties were repeated for five times and average values were taken. The weight residue (%) of bentonite and modified bentonite clay and thermal stability of the nanocomposites were measured by thermogravimetric analysis (TGA) in Shimazdu TG 50 using nitrogen flow rate of 30 mL/min at the heat rate of 10°C/min from room temperature to 700°C. The experimental tensile modulus values (calculated from elastic region of the stress–strain profiles) of the nanocomposites were compared with the predicted values calculated from (1) Guth generalized Einstein's equation:[26,27]

$$E_{NC} = E_M\left[1 + K_E V_f + 14.1\left(V_f\right)^2\right] \quad (1)$$

and

(2) Halpin–Tsai (a) random model:[28–30]

$$E_{NC} = E_M\left[(3/8)\left\{\left(1+\eta_L\xi V_f\right)/\left(1 - \eta_L V_f\right)\right\} + (5/8)\left\{\left(1+2\eta_T V_f\right)/\left(1 - \eta_T V_f\right)\right\}\right] \quad (2)$$

and (b) aligned parallel model:[28–30]

$$E_{NC} = E_M\left[\left(1+\eta_L\xi V_f\right)/\left(1-\eta_L V_f\right)\right] \quad (3)$$

where

$$\eta_L = \left[\left(E_{NP}/E_M - 1\right)/\left(E_{NP}/E_M + \xi\right)\right] \quad (4)$$

and

$$\eta_T = \left[\left(E_{NP}/E_M - 1\right)/\left(E_{NP}/E_M + 2\right)\right] \quad (5)$$

Here, E_{NC} is the tensile modulus of the nanocomposites, E_M is the tensile modulus of the matrix, K_E is the Einstein's coefficient

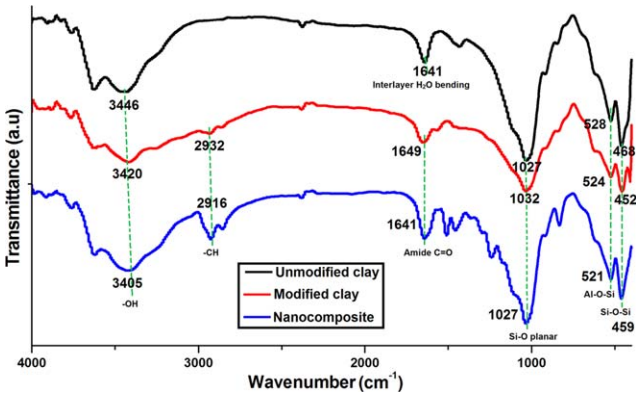

Figure 2. FTIR spectra of pristine bentonite, modified bentonite and MNC3. [Color figure can be viewed in the online issue, which is available at wileyonlinelibrary.com.]

which is 0.67ξ (ξ is length to thickness ratio of clay) and V_f is the volume fraction of the clay. The experimental modulus values were measured as slops of the linear portion (1–2% strain) of the stress–strain curves. The equation used for this purpose is $y = mx + c$, where m (modulus) is the slope, y is stress, and x is strain.

RESULTS AND DISCUSSION

Modification and Characterization of Bentonite Clay

The hydrophilic bentonite clay was modified by alkyl ammonium ion exchange process. Na^+ ions of hydrophilic bentonite clay were exchanged by aliphatic poly(amido-ammonium) ion. The characteristic diffraction peak shifted from $2\theta = 7.1°$ to 4.9° after modification [Figure 1(a)]. Thus basal spacing increases 0.56 nm after modification as calculated from XRD data by Bragg's equation. This is due to the fact that the clay layers are intercalated by the branched structure of poly(amido-amine) modifying agent. In FTIR spectrum of modified clay (Figure 2), the bands at 2932 cm^{-1} indicated the presence of aliphatic —CH_2 stretching band. The others bands were observed at 3420, 1649, 1560, 1032, 524, and 452 cm^{-1} confirmed the presence of —NH and —OH, amide (C═O), interlayer H_2O, Si—O, Al—O—Si, Si—O—Si groups respectively. But in case of unmodified bentonite clay the band at 2932 cm^{-1} was absent. The —OH stretching frequency of unmodified clay at 3446 cm^{-1} was diminished with broad nature at 3420 cm^{-1} in modified clay. The interlayer H_2O bending of unmodified clay at 1641 cm^{-1} was also diminished and shifted to 1565 cm^{-1} in modified clay. The hydrophobicity of the modified clay on incorporation of aliphatic poly(amido-amine) was also indirectly confirmed by TGA analysis, as no significant weight loss was observed near 100°C. The thermograms of pristine and modified bentonite clay are shown in Figure 3(a). A continuous weight loss (11%) up to 100°C of pristine bentonite was observed, which was almost insignificant (2%) for modified system. This weight loss is due to the loss of structural and absorbed water molecules. Again, the unmodified hydrophilic bentonite was thermally more stable and the weight residue found at 700°C was 85%, while modified clay was continuously lost its weight and 78% weight residue was remained at 700°C. This continuous and gradual loss of weight in the modified system is due to the degradation of aliphatic hydrocarbon of poly(amido-amine).

Preparation and Characterization of the Nanocomposites

The hyperbranched epoxy/modified clay nanocomposites were prepared by solution technique using mechanical shearing force and ultra-sonication. The curing time was optimized by swelling value and the optimum cure time was taken at swelling value of 20–25% (75% gel fraction). The result of swelling values for MNC0, MNC1, MNC3, and MNC5 was almost equivalent (22, 19, 21, and 22%). Thus, the crosslink density is almost equal. The optimum curing time of the nanocomposites with 50% poly(amido-amine) at 100°C decreases with the increases of clay content in the nanocomposites (Table I). This is due to the strong interaction of hyperbranched epoxy with the modified clay. The aliphatic poly(amido-amine) of the modified clay also took part in crosslinking reaction with the hyperbranched epoxy.

The diffraction peak for d_{001} of the modified clay at $2\theta = 4.9°$ was completely diminished in nanocomposites as observed in

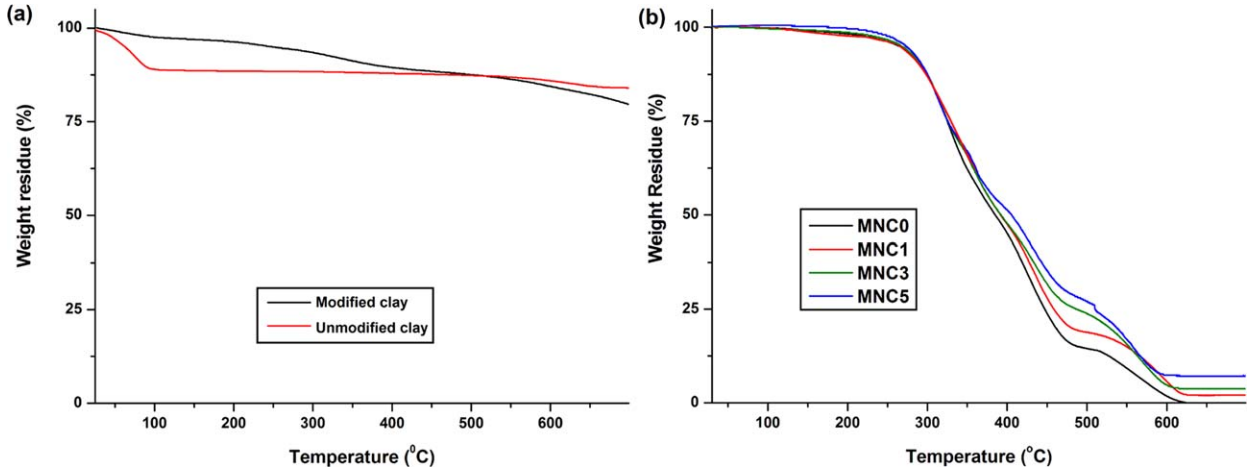

Figure 3. (a) TGA thermograms of pristine and modified bentonite and (b) TGA thermograms of pristine epoxy thermoset and nanocomposites. [Color figure can be viewed in the online issue, which is available at wileyonlinelibrary.com.]

Table I. Performance of the Nanocomposites

Properties	MNC0	MNC1	MNC3	MNC5	BNC3	SBE[e]
Curing time at 100°C (min)	80	70	55	45	90	75
Swelling value (%) at 25°C	22	19	21	22	34	21
Tensile strength (MPa)	38.5 ± 1	46 ± 2	57 ± 4	41 ± 1	17.5 ± 2	38 ± 1
Elongation at break (%)	16.5 ± 1	33.5 ± 2	43 ± 1.5	54 ± 3	55 ± 4	5 ± 0.5
Toughness	252 ± 12	897 ± 8	1804 ± 14	1626 ± 17	827 ± 7	143 ± 8
Impact resistance[a] (cm)	>100	>100	>100	>100	95	65
Scratch hardness[b] (kg)	9.0	>10.0	>10.0	>10.0	8.5	7.0
Bending dia[c] (mm)	<1	<1	<1	<1	<1	>4
Adhesive strength[d] (W-W) (MPa)	2680 ± 30	4348 ± 20	4393 ± 40	4414 ± 15	3422 ± 40	944 ± 12
Adhesive strength (M-M) (MPa)	2662 ± 15	6698 ± 18	6748 ± 12	6740 ± 16	3658 ± 22	822 ± 9

[a] The limit of the impact strength was 100 cm (highest).
[b] The limit of the scratch hardness was 10.0 kg (highest).
[c] The limit of the mandrel diameter was 1 mm (lowest).
[d] In all the nanocomposites wood substrate was failed.
[e] The data for standard bisphenol-A based epoxy thermoset are reproduced from our earlier work just for comparison purpose for better understanding.[4,34]

XRD patterns [Figure 1(b)]. This may be due to the intercalation of polymer chain into the clay layers and also strong interactions like hydrogen bonding, polar-polar interactions, etc. which facilitate the well dispersions of clay layers with the epoxy. The presence of Si—O planar stretching and, Al—O—Si and Si—O—Si bending of the clay in nanocomposites was confirmed by the FTIR bands at 1027 and, 521 and 459 cm^{-1} respectively (Figure 2). The shifting of —OH band of modified clay in nanocomposites from 3420 to 3405 cm^{-1} is due to the different physicochemical interactions of clay with the hyperbranched epoxy. The TEM image discloses the actual picture of state of dispersion of clay in the nanocomposites. Figure 4(a) reveals the homogenous dispersion of disordered structure of clay layers in the epoxy matrix. The image shows both the exfoliation and intercalation of clay layers in hyperbranched epoxy matrix. SEM is also a valuable technique for examining the morphology of the nanocomposites. Uniform dispersion of clay in the hyperbranched epoxy was also confirmed by the SEM image of the fracture surface of the nanocomposite [Figure 4(b)]. This uniform dispersion is due to the strong physicochemical interactions of aliphatic poly(amido-amine) of modified clay with hyperbranched epoxy and the hardener as shown like in the Scheme 1.

Mechanical Properties of the Nanocomposites

The mechanical properties of the nanocomposites with different amount of clay loading were given in the Table I. The interesting results in this study were the achievement of excellent toughness and high flexibility of the nanocomposites. The toughness of the nanocomposites as determined by integrating the stress–strain curves was sharply increased with the increase of amount of clay and thus the nanocomposites behave like

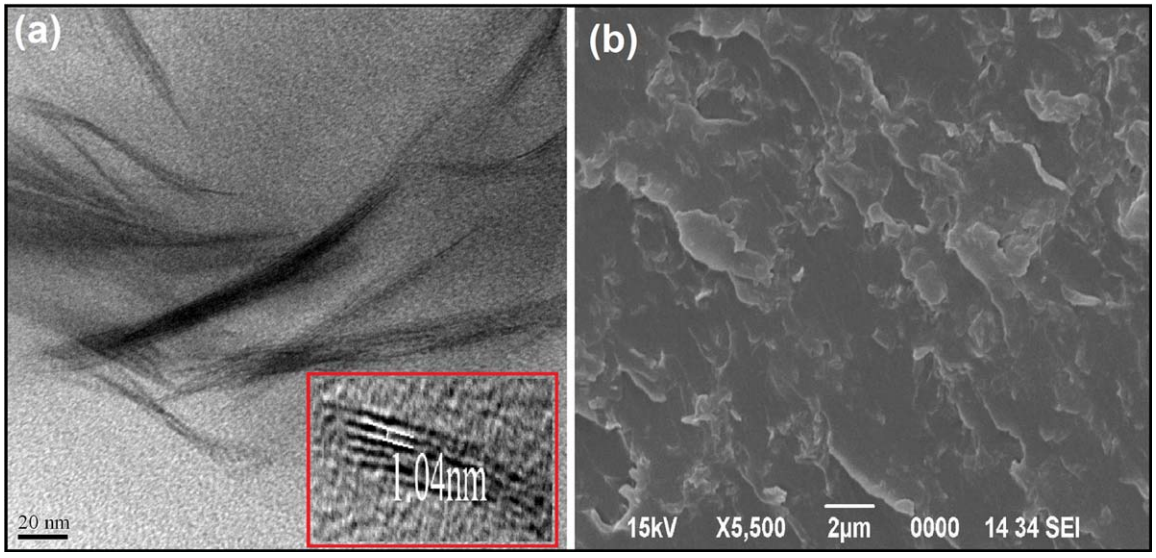

Figure 4. (a) TEM and (b) SEM images of MNC3. [Color figure can be viewed in the online issue, which is available at wileyonlinelibrary.com.]

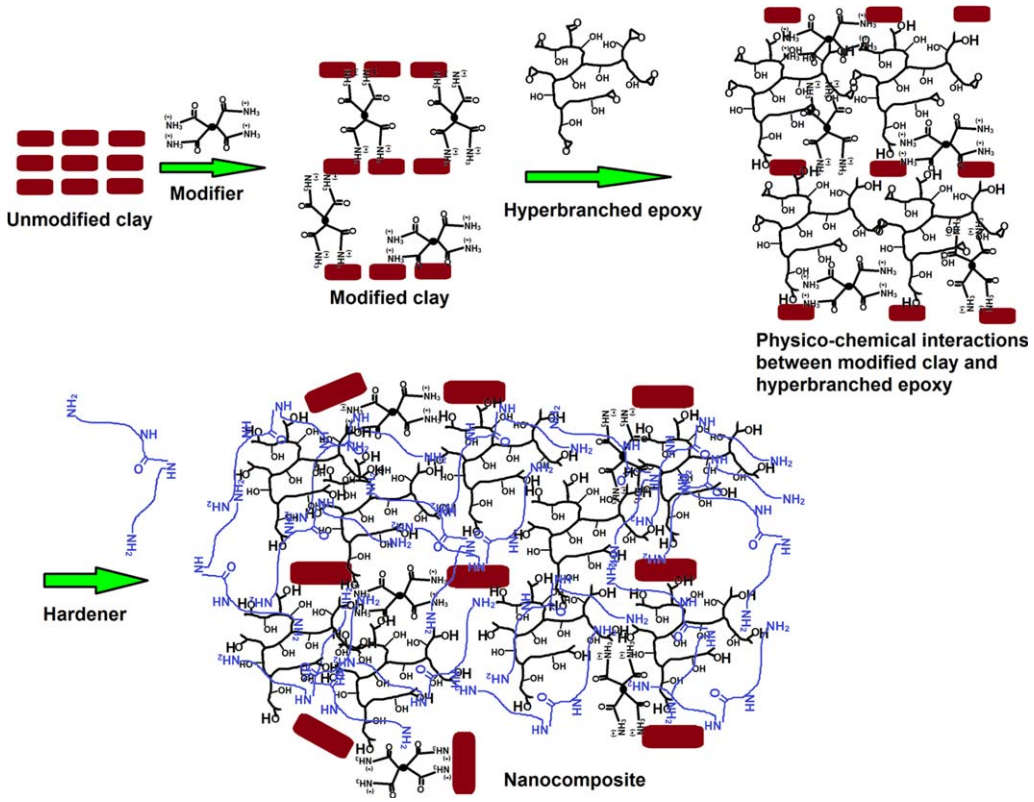

Scheme 1. Different physicochemical interactions of modified clay with hyperbranched epoxy and hardener based on the H–T aligned parallel model. [Color figure can be viewed in the online issue, which is available at wileyonlinelibrary.com.]

ductile materials. This is the combined effects of the flexible hydrocarbon chains of the aliphatic poly(amido-amine), the modifying agent; different flexible moieties of hyperbranched epoxy, and the long chain hydrocarbon part of the fatty acid of poly(amido-amine) hardener with the aromatic rigid moiety and clay platelets. The plasticizing effect of these flexible moieties has definite role for the above results. Again, both hyperbranched epoxy and poly(amido-amine) help to increase the free volume between the molecules because of the steric effect.[1,33] It is also possible that clay platelets act as both physical and chemical crosslinkers (Scheme 1).[20] Both platelet motion and long range intercalations through physical crosslinks are potential candidates for the observed toughening of hyperbranched epoxy. The elongation at break was sharply increased with the increase of the amount of clay loading (Figure 5). It has been proposed that the increased elongation at break of polymer–clay nanocomposites may result from the mobility of exfoliated clay platelets, which provides a mode for

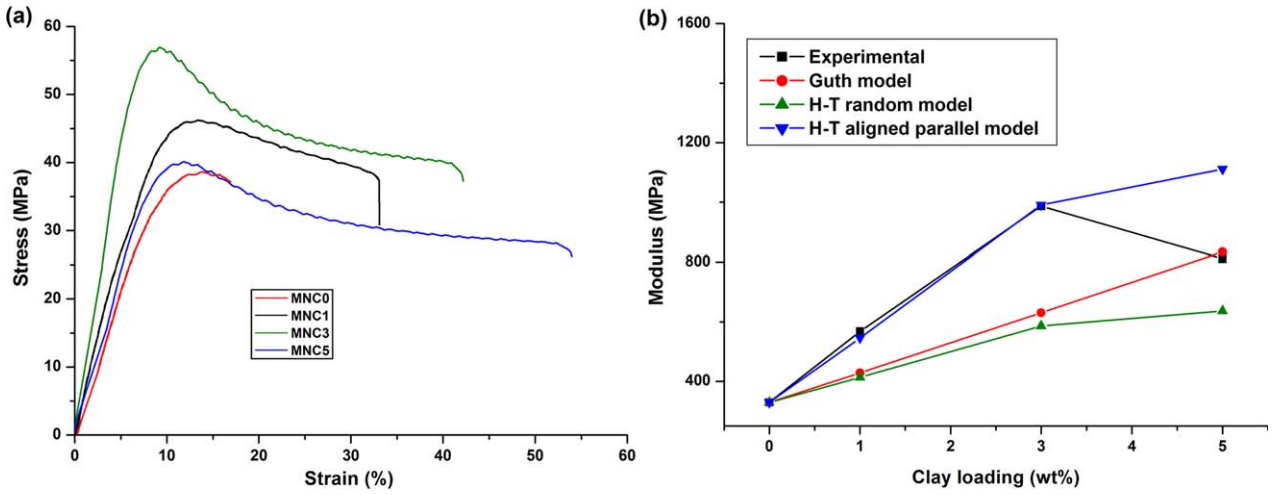

Figure 5. (a) Stress–strain profiles of pristine hyperbranched epoxy thermoset and nanocomposites, (b) plots of tensile modulus of predicted and experimental values of nanocomposites. [Color figure can be viewed in the online issue, which is available at wileyonlinelibrary.com.]

Table II. Predicted and Experimental Modulus Values (Mpa)

Mechanical models	MNC0	MNC1	MNC3	MNC5
Guth generalized Einstein equation	329	428	630	834
Halpin–Tsai random model	329	413	586	637
Halpin–Tsai aligned parallel model	329	546	991	1111
Experimental value[a]	329	568	987	807

[a] Calculated from stress–strain curve.

energy dissipation.[20] The tensile strength value of the hyperbranched epoxy thermoset was increased on incorporation of clay up to 3 wt % of loading, though the same was almost remained unchanged at 5 wt % loading. This is due to the agglomeration of clay particles in the polymer matrix at high loading. The impact strength and scratch hardness were also very high for the nanocomposites. The nanocomposites were exhibited high flexibility as they bent up to the lowest diameter of a mandrel (1 mm) or 180° without any damage or fracture for the same reason. As both the nanocomposites and the pristine epoxy were reached the highest limit of the instrument of the impact resistance (100 cm) and flexibility (1 mm), the enhancement of these values could not determine. The nanocomposites were also reached the highest limit of the instrument of the scratch hardness value (10.0 kg). To account the polymer–filler interactions and for prediction of the modulus of the nanocomposites Guth generalized Einstein equation and Halpin–Tsai (H–T) random and aligned parallel mechanical models were used [Figure 5(b)]. The experimental modulus values of the nanocomposites were matched with the Halpin–Tsai (H–T) aligned parallel mechanical model [Figure 5(b) and Table II] at low amount of clay content (1 and 3 wt %). However, at high amount of clay content (5 wt %) the experimental modulus value was deviated from this model. This is due to the aggregation of clay platelet in the matrix at high amount of clay content. But at high amount of clay content (5 wt %) the experimental modulus value was matched with the Guth model [Figure 5(b)]. This is due to the fact that the Guth model only considered electrostatic and van der Walls interactions (physical interactions) between the fillers and the matrix.[26] However as in MNC1 and MNC3 both physical and chemical interactions are present their experimental modulus values are much higher compared to the Guth model (Table II).

Adhesive Strength of the Nanocomposites

Two fold improvement in adhesive strength with both wood–wood (W–W) and metal–metal (M–M) substrates was found after formation of nanocomposites (Table I). This is due to the presence of highly polar oxygen and nitrogen containing groups of epoxy, hardener, and clay, which help to generate strong interaction with the cellulosic wood substrates. The branched architecture of hyperbranched epoxy, poly(amido-amine), and clay nanoparticles also help to physical interlocking with the metal substrates. The diffusion of clay dispersed hyperbranched epoxy and hardener into the metal substrates helps to strong physical interlocking.

Thermal Stability

Slight increment in thermal stability and weight residue was observed in the TGA thermograms [Figure 3(b)] after formation of nanocomposites. This is due to the presence of large numbers of aliphatic moieties of hyperbranched epoxy, hardener and aliphatic poly(amido-amine). Only different physicochemical interactions of the matrix and the modifying agent with the clay platelets slightly improve the thermal stability. However, the weight residues of nanocomposites were increased due to the presence of clay platelets, which are thermostable at 700°C.

Performance of Hyperbranched Epoxy/Unmodified Bentonite Nanocomposite and Standard Bisphenol-A Based Epoxy Thermoset

The nanocomposite of hyperbranched epoxy with 3 wt % of unmodified bentonite clay was also prepared by using the same procedure and coded as BNC3. But due to the very poor interactions, the clay particles were separated out from the hyperbranched epoxy matrix and thus exhibited low performance (Table I). This is due to the hydrophilic nature of the unmodified clay resulted high moisture absorption and less compatibility with the epoxy matrix and thus they agglomerate inside the matrix. Performance of the hyperbranched epoxy and the nanocomposite thermosets are also compared with the standard bisphenol-A based epoxy cured by the same poly(amido-amine) hardener (SBE) as reported earlier.[4,34] Table I clearly indicates better performance of hyperbranched epoxy thermoset than the SBE. MNC3 showed the highest performance among the studied nanocomposites with 12.6- and 8-folds greater toughness and elongation at break, respectively than SBE. It also exhibited 50 and 700% higher tensile strength and adhesive strength, respectively, than SBE.

CONCLUSIONS

An outstanding tough and flexible hyperbranched epoxy and aliphatic poly(amido-amine) modified bentonite based thermosetting nanocomposite with high elongation at break and adhesive strength was demonstrated. A significant improvement in toughness was observed from the area under the stress–strain curve. The simultaneous increment in tensile strength and elongation at break resulted in ductility of the nanocomposites and is a commendable achievement, which was not found so far. Thus this study may provide a new insight into the epoxy/clay nanocomposites for their future exploration. The unique characters like high strength, toughness, and ductility render the nanocomposites as highly potential materials for engineering applications.

ACKNOWLEDGMENTS

The authors express their gratitude to the NRB for financial assistance through the grant no. DNRD/05/4003/NRB/251 dated 29.02.12, SAP (UGC), India through grant no. F.3-30/2009 (SAPII) and the FIST program-2009 (DST), India through the grant no. SR/FST/CSI-203/209/1 dated 06.05.2010. SAIF of NEHU, Shillong is gratefully acknowledged for the TEM imaging.

REFERENCES

1. De, B.; Karak, N. *J. Mater. Chem. A* **2013**, *1*, 348.
2. Lee, H.; Neville, K. Handbook of Epoxy Resins; McGraw-Hill: New York, **1967**.
3. Barua, S.; Dutta, G.; Karak, N. *Chem. Eng. Sci.* **2013**, *95*, 138.
4. De, B.; Voit, B.; Karak, N. *ACS Appl. Mater. Interfaces* **2013**, *5*, 10027.
5. Zhang, D.; Jia, D. *J. Appl. Polym. Sci.* **2006**, *101*, 2504.
6. Ratna, D.; Varley, R.; Simon, GP. *J. Appl. Polym. Sci.* **2003**, *89*, 2339.
7. Feast, W. J.; Wang, X. *Chin. J. Polym. Sci.* **2002**, *20*, 585.
8. Lan, T.; Pinnavaia. T. *J. Chem. Mater.* **1994**, *6*, 2216.
9. Deng, F.; Vliet, K. J. V. *Nanotechnology* **2011**, *22*, 165703.
10. Park, I.; Peng, H.; Gidley, D. W.; Xue, S.; Pinnavaia, T. *J. Chem. Mater.* **2006**, *18*, 650.
11. Park, J. H.; Jana, S. C. *Macromolecules* **2003**, *36*, 2758.
12. Chen, B.; Evans, J. R. G.; Greenwell, H. C.; Boulet, P.; Coveney, P. V.; Bowden, A. A.; Whiting, A. *Chem. Soc. Rev.* **2008**, *37*, 568.
13. Wang, K.; Chen, L.; Wu, J.; Toh, M. L.; He, C.; Yee, A. F. *Macromolecules* **2005**, *38*, 788.
14. Bragancua, F. C.; Valadares, L. F.; Leite, C. A. P.; Galembeck, F. *Chem. Mater.* **2007**, *19*, 3334.
15. Jagtap, S. B.; Rao, V. S.; Ratna, D. *J. Reinf. Plast. Compos.* **2012**. doi:10.1177/0731684412462916.
16. Lopez, D. G.; Mitre, I. G.; Fernandez, J. F.; Merino, J. C.; Pastor, J. M. *Polymer* **2005**, *46*, 2758.
17. Khoeini, M.; Bazgir, S.; Tamizifar, M.; Nemati, A.; Arzani, K. *Ceram. Silikaty.* **2009**, *53*, 254.
18. Wang, W. S.; Chen, H. S.; Wu, Y. W.; Tsai, T. Y.; Chen-Yang, Y. W. *Polymer* **2008**, *49*, 4826.
19. Kornmanna, X.; Lindbergb, H.; Berglund, L. A. *Polymer* **2001**, *42*, 1303.
20. Wang, J.; Severtson, S. J.; Stein, A. *Adv. Mater.* **2006**, *18*, 1585.
21. Shah, D.; Maiti, P.; Gunn, E.; Schmidt, D. F.; Jiang, D. D.; Batt, C. A.; Giannelis, E. P. *Adv. Mater.* **2004**, *16*, 1173.
22. Liu, W.; Hoa, S. V.; Pugh, M. *Compos. Sci. Technol.* **2005**, *65*, 307.
23. Zerda, A. S.; Lesser, A. J. *J. Polym. Sci. Part B: Polym. Phys.* **2001**, *39*, 1137.
24. Wang, L.; Wang, K.; Chen, L.; Zhang, Y.; He, C. *Composit. Part A* **2006**, *37*, 1890.
25. Balakrishnan, S.; Start, P. R.; Raghavan, D.; Hudson, S. D. *Polymer* **2005**, *46*, 11255.
26. Kumar, P.; Sandeep, K. P.; Alavi, S.; Troung, V. D. *J. Food. Sci.* **2011**, *76*, E2.
27. Ahmed, S.; Jones, S. R. *J. Mater. Sci.* **1990**, *25*, 4933.
28. Rafiee, M. A.; Rafiee, J.; Wang, Z.; Song, H.; Yu, Z. Z.; Koratkar, N. *Acs Nano* **2009**, *3*, 3884.
29. Thakur, S.; Karak, N. *RSC Adv.* **2013**, *3*, 9476.
30. Ramakrishna, S.; Lim, T. C.; Inai, R.; Fujihara, K. *Mech. Adv. Mater. Struct.* **2006**, *13*, 77.
31. Tomalia, D. A.; Dewald, J. R. *US Pat.* 4,568,737, **1986**.
32. Yiyun, C.; Dazhu, C.; Rongqiang, F.; Pingsheng, H. *Polym. Int.* **2005**, *54*, 495.
33. Yang, J. P.; Chen, J. K.; Yang, G.; Fu, S. Y.; Ye, L. *Polymer* **2008**, *49*, 3168.
34. De, B.; Gupta, K.; Mandal, M.; Karak, N. *ACS Sustain. Chem. Eng.* **2013**. doi:10.1021/sc400358b.